HHS Public Access
Author manuscript
Nature. Author manuscript; available in PMC 2018 April 25.

Releasing Ski-Smad4 mediated suppression is essential to license Th17 differentiation

Song Zhang[1,2], **Motoki Takaku**[3], **Liyun Zou**[1,2], **Ai-di Gu**[1,2], **Wei-chun Chou**[1,2,4], **Ge Zhang**[1,2,5], **Bing Wu**[1,2], **Qing Kong**[1,2,6], **Seddon Y. Thomas**[7], **Jonathan S. Serody**[1,2], **Xian Chen**[1,6], **Xiaojiang Xu**[8], **Paul A. Wade**[3], **Donald N. Cook**[7], **Jenny P. Ting**[1,2,4], and **Yisong Y. Wan**[1,2,*]

[1]Lineberger Comprehensive Cancer Center, University of North Carolina at Chapel Hill, NC, 27599

[2]Department of Microbiology and Immunology, University of North Carolina at Chapel Hill, NC 27599

[3]Epigenetics and Stem Cell Biology Laboratory, National Institute of Environmental Health Sciences, Research Triangle Park, NC 27709

[4]Department of Genetics, University of North Carolina at Chapel Hill, NC, 27599

[5]Dalian Medical University, Dalian 116044, China

[6]Department of Biochemistry and Biophysics, University of North Carolina at Chapel Hill, NC 27599

[7]Immunity, Inflammation, and Disease Laboratory, Division of Intramural Research, National Institute of Environmental Health Sciences, National Institutes of Health, Research Triangle Park, NC 27709

[8]Integrative Bioinformatics, National Institute of Environmental Health Sciences, Research Triangle Park, NC 27709

Abstract

Th17 cells are critically involved in host defense, inflammation, and autoimmunity[1–5]. TGF-β is instrumental in Th17 differentiation by cooperating with IL-6[6,7]. Yet, the mechanism of how TGF-β enables Th17 differentiation remains elusive. Here we reveal that TGF-β licenses Th17

*Correspondence and requests for materials should be addressed to wany@email.unc.edu.

Supplementary Information is linked to the online version of the paper at www.nature.com/nature.

differentiation by releasing Ski-Smad4-complex suppressed RORγt expression. We found serendipitously that, unlike wild-type T cells, Smad4-deficient T cells differentiated into Th17 cells in the absence of TGF-β signaling in a RORγt-dependent manner. Ectopic Smad4 expression suppressed the RORγt expression and Th17 differentiation of Smad4-deficient T cells. Unexpectedly however, TGF-β neutralized Smad4 mediated suppression without affecting Smad4 binding to *Rorc* locus. Proteomic analysis revealed that Smad4 interacted with Ski, a transcriptional repressor degraded upon TGF-β stimulation. Ski controlled the histone acetylation/de-acetylation of *Rorc* locus and Th17 differentiation via Smad4 because ectopic Ski expression inhibited H3K9Ac of *Rorc* locus, *Rorc* expression and Th17 differentiation in a Smad4-dependent manner. Therefore, TGF-β-induced disruption of Ski releases Ski-Smad4 complex imposed suppression of RORγt to license Th17 differentiation. This study reveals a critical mechanism by which TGF-β controls Th17 differentiation and uncovers Ski-Smad4 axis as a potential therapeutic target for treating Th17 related diseases.

We studied the mechanisms underlying the important role for TGF-β signaling in Th17 differentiation[6–10]. We found that CD4^{+} T cells from wild-type and *Cd4cre;Smad4*^{fl/fl} mice[11] differentiated into Th17 cells comparably in the presence of IL-6 and TGF-β, as reported previously[12]. However, in stark contrast to wild-type T cells, Smad4-deficient T cells consistently differentiated into Th17 cells when provided with IL-6 alone without TGF-β (Fig. 1a). This observation prompted us to hypothesize that Smad4 deletion may result in Th17 cell differentiation in the absence of TGF-β signaling. To test this hypothesis, we blocked TGF-β signaling effectively by using a pharmacological inhibitor for TGF-β receptor (TGFβR) kinase activity. Strikingly, while wild-type T cells did not become Th17 cells, Smad4-deficient T cells readily differentiated into Th17 cell and expressed Th17 related genes when TGF-β signaling was inhibited (Fig. 1a, b and Extended Data Fig. 1a). To confirm this finding and rule out the potential off-target effect of the inhibitor, we generated *Cd4cre;Smad4*^{fl/fl}*;Tgfbr2*^{fl/fl} (S4-RII DKO) mice, where both Smad4 and TGF-β receptor II (TGFβRII) were deleted specifically in T cells[11,13–15]. In agreement with the results of the experiments using the TGFβR inhibitor, Smad4 and TGFβRII double knockout CD4^{+} T cells effectively differentiated into Th17 cells when only IL-6 was provided (Fig. 1c, 1d).

Intrigued by the findings obtained *in vitro*, we further investigated if Smad4-deficient T cells could differentiate into Th17 cells in the absence of TGF-β signaling *in vivo*. Under steady state, S4-RII DKO mice had comparable, if not slightly higher, percentages of Th17 cells when compared to wild-type mice, while virtually no Th17 cells were detected in *Cd4cre;Tgfbr2*^{fl/fl} mice (Extended Data Fig. 1b). We then addressed if S4-RII DKO T cells could differentiate into Th17 cells during experimental autoimmune encephalomyelitis (EAE) development. S4-RII DKO T cells differentiated into Th17 cells as effectively as wild-type T cells (Fig. 1e) upon EAE elicitation. S4-RII DKO mice developed EAE and associated pathology (Fig. 1f, g). In addition, by using a tamoxifen inducible ERCre system[16], we found that acute deletion of Smad4 enabled Th17 cell differentiation in the absence of TGFβRII, although TGFβRII-deficient T cells failed to differentiate into Th17 cells under the same conditions (Fig. 1h). These findings therefore demonstrated that

Smad4-deficient T cells can differentiate into pathological Th17 cells in the absence of TGF-β signaling.

We next investigated how Smad4 deletion impacted the molecular program controlling Th17 differentiation. The expression of many Th17 cell related genes was dramatically increased in Smad4-deficient T cells when compared to wild-type T cells, as early as one day post activation when only IL-6 was provided (Extended Data Fig. 2a). To identify the primary target of Smad4 for Th17 differentiation, we compared gene expression in wild-type and Smad4-deficent T cells at the very early time points. While the expression of many Th17 related genes was undetectable or showed insignificant difference between wild-type and Smad4-deficient T cells, *Rorc* expression was prominently and drastically increased in Smad4-deficient T cells within 12 hours of activation in the presence of IL-6 and TGFβR inhibitor (Fig. 2a and Extended Data Fig. 2b, c). Such an elevated *Rorc* expression was similarly observed in S4-RII DKO T cells (Extended Data Fig. 2d). The RORγt protein expression agreed with the *Rorc* mRNA expression in both S4 KO and S4-RII DKO T cells (Extended Data Fig. 2e, f). These results strongly suggested an involvement of RORγt in Smad4 controlled Th17 cell differentiation. Indeed, deletion of RORγt in Smad4-deficient T cells abolished their Th17 differentiation in the absence of TGF-β (Fig. 2b).

We then addressed if adding back Smad4 into Smad4-deficient T cells can restore their function to be like wild-type cells. Indeed, retrovirus mediated ectopic Smad4 expression inhibited the Th17 differentiation of Smad4-deficient T cells in the absence of TGF-β (Fig. 2c, d). Smad4 suppressed the expression of *Rorc* preceding other Th17 related genes (Fig. 2e). In addition, *Rorc* was a functionally critical Smad4 target because ectopic RORγt expression overcame Smad4 suppressed Th17 differentiation in the absence of TGF-β signaling (Fig. 2f). Smad4 appeared to suppress Th17 differentiation via a direct mechanism on *Rorc* expression, because Smad4 bound to multiple sites in *Rorc* locus including the promoter region (Fig. 2g and Extended Data Fig. 2g) but not to *Il17a or Il17f* loci (Extended Data Fig. 2h).

Based on the findings described above, one may further predict that ectopic Smad4 expression will also suppress RORγt expression and Th17 differentiation in the presence of both IL-6 and TGF-β (the classic Th17 cell polarizing condition). Quite to the contrary however, addition of TGF-β abolished the ability of Smad4 to suppress Th17 differentiation (Fig. 3a). The findings suggest that one important mechanism through which TGF-β enables Th17 differentiation is to overcome Smad4 mediated suppression. TGF-β may do so by dislodging Smad4 from *Rorc* locus. It was however not the case because Smad4 remained bound to *Rorc* locus regardless TGF-β's presence (Fig. 3b). Another possibility is that TGF-β signaling alters Smad4's interaction with other proteins, because associating with different factors is an important means for Smad4 function[17]. We developed a screening strategy based on quantitative proteomics[18] (Extended Data Fig. 3a) to identify proteins that preferentially bound to Smad4 in the absence but not in the presence of TGF-β signaling in activated T cells. Ski, a factor whose deregulation tightly associates with tumorigenesis, 1p36 deletion syndrome and Shprintzen-Goldberg syndrome[19–21], was identified by this approach. Such a differential interaction between Smad4 and Ski was validated by immuno-precipitation assays (Fig. 3c). Ski is degraded upon TGF-β signaling in cancer cells[22].

Similarly in T cell, very low dose of TGF-β stimulation during Th17 differentiation induced a drastic Ski protein down-regulation that was partially Smad2- and Smad3-dependent (Fig. 3d and Extended Data Fig. 3b, c, d), associating with a much shortened Ski half-life (Fig. 3e). We then investigated if Ski-Smad4 interaction is important for Smad4 mediated suppression of Th17 differentiation. Indeed, Smad4 mutants[23] that are defective in interacting with Ski failed to suppress Th17 differentiation of Smad4-deficient T cells in the absence of TGF-β (Fig. 3f, g).

The aforementioned findings promoted us to test how Ski expression may impact Th17 differentiation. We ectopically expressed Ski to maintain its expression in the presence of both IL-6 and TGF-β. Ski expression potently suppressed Th17 differentiation (Fig. 4a) with a prompt suppression of *Rorc* expression *in vitro* (Fig. 4b). Similarly *in vivo*, T cells that ectopically expressed Ski were defective in differentiating into Th17 cell during EAE development (Fig. 4c). In addition, disruption of Ski expression enabled CD4^{+} T cells to differentiate into Th17 cells in the absence of TGF-β (Extended Data Fig. 4a). These findings suggest that Ski functions downstream of TGF-β to inhibit *Rorc* expression and Th17 differentiation. Indeed, ectopic RORγt expression restored the Th17 differentiation of Ski-expressing cells (Extended Data Fig. 4b). Smad4 is critical to mediate Ski function because ectopic Ski expression failed to suppress the Th17 differentiation of cells that were Smad4 deficient (Fig. 4d). Therefore, Ski and Smad4 interact and cooperate to suppress *Rorc* expression and to restrain Th17 differentiation.

We further investigated the mechanism through which the Ski-Smad4 axis suppresses *Rorc* expression. Because Ski recruits HDACs to repress gene expression[24], we studied how Ski-Smad4 axis may regulate the histone acetylation of *Rorc* locus. As expected, H3K9 acetylation in the *Rorc* promoter region was substantially elevated under Th17 polarizing condition in a TGF-β-dependent manner in wild-type T cells (Fig. 4e). Nonetheless, Smad4 deletion led to H3K9 acetylation of *Rorc* promoter region in the absence of TGF-β (Fig. 4e). Importantly, ectopic Ski expression suppressed the acetylation of H3K9 of *Rorc* promoter region in wild-type but not in Smad4-deficient T cells (Fig. 4f). In addition, we found that Ski bound to *Rorc* promoter at the same site as Smad4 in a Smad4- and TGF-β-dependent manner (Extended Data Fig. 4c). These findings suggest that Ski-Smad4 complex directly regulates the histone acetylation of *Rorc* locus to suppress RORγt expression.

The aforementioned findings collectively suggest that in the absence of TGF-β, Ski-Smad4 complex binds to and modifies the histone acetylation/deacetylation of *Rorc* locus to repress RORγt expression. Yet, TGF-β stimulation leads to Ski degradation to release Ski-Smad4 repressed *Rorc* expression and to license Th17 differentiation (Extended Data Fig. 5). Since TGF-β superfamily members share many common signaling pathways, we tested if other family members can also promote Ski degradation and Th17 differentiation. Indeed, we found that Activin, a cytokine that activates signaling pathways similar to those activated by TGF-β[25], induced Ski degradation in activated T cells (Fig. 4g) and promoted Th17 differentiation (Fig. 4h). Importantly, ectopic Ski expression potently suppressed Activin-promoted Th17 differentiation (Fig. 4i). In addition, Smad4 was required for Ski mediated suppression of Th17 differentiation induced by Activin (Fig. 4j). Therefore, Ski-Smad4 complexes relay diverse upstream signals to regulate Th17 differentiation.

Given the vital roles for Th17 cells in normal physiology and myriad diseases, it is important to understand how these cells are generated. Both IL-6 and TGF-β signaling are instrumental in the induction of Th17 cells[6,7]. Although IL-6/STAT3 signaling potentiates RORγt expression[26–28], it is insufficient for Th17 differentiation; TGF-β signaling is also required[6,7]. In the current study, we revealed Ski as a potent Th17 suppressor whose function relies on Smad4 to restrain RORγt expression. Importantly, we discovered that a central function of TGF-β for Th17 differentiation is to degrade Ski, hence to release Ski-Smad4 restrained *Rorc* expression to license Th17 differentiation. These findings not only shed light on how Th17 cell differentiation is controlled, but also uncover Ski-Smad4 axis as a critical molecular target to interfere with Th17 function for treating related immune diseases.

METHODS (Online Information)

Mice

Smad4^{fl/fl}, *Tgfbr2*^{fl/fl}, *Cd4cre*, *ERCre*, *Rag1*^{−/−}, *Rorc*^{−/−}, Cre-dependent-Cas9 knockin (CdC)[29] and CD45.1 congenic wild-type mice were on the C57BL/6 background. Littermates were used unless stated otherwise. All mice were housed and bred in specific pathogen–free conditions in the animal facility at the University of North Carolina at Chapel Hill. All mouse experiments were approved by Institution Animal Care and Use Committee of the University of North Carolina. We have complied with all relevant ethical regulations.

Flow cytometry and cell sorting

Lymphocytes were isolated from various organs of 6–18 weeks old, age- and sex-matched mice of. Fluorescence-conjugated anti-CD4 (GK1.5), anti-CD25 (PC61.5), anti-CD62L (MEL-14), anti-CD44 (IM7), anti-CD45.1 (A20), anti-CD45.2 (104), anti-IFN-γ (XMG1.2), anti-Thy1.1 (OX-7) and anti-IL-17A (TC11-18H10.1) (Biolegend) were used. For intracellular cytokine staining, lymphocytes were stimulated for 4 hours with 50ng/ml of PMA (phorbol 12-myristate 13-acetate) and 1μM ionomycin in the presence of brefeldin A. Stained cells were analyzed on a FACSCanto (BD Biosciences) or were sorted on a MoFlo (DakoCytomation, Beckman Coulter). A figure exemplifying the gating strategy is provided in Supplementary Fig. 2.

T cell culture and differentiation

Naïve (CD4+CD25−CD44^{low}CD62L^{high}) T cells were sorted from the peripheral lymph nodes and spleens of mice. Cells were then activated either in plates coated with 10μg/ml anti-CD3 (145-2C11, BioXCell) and 10μg/ml anti-CD28 (37.51, BioXCell) or by soluble 1μg/ml anti-CD3 and irradiated (3000 cGy) T-cell-depleted splenocytes. Cells were cultured in RPMI medium with 10% FBS and 1% antibiotics unless specifically indicated. Cells were cultured in the presence of 20μg/ml anti-IFN-γ (XMG1.2, BioXcell) and 20μg/ml anti-IL-4 (11B11, BioXcell). For IL-6+TGF-β condition, cells were cultured in the presence of 40ng/ml recombinant IL-6, 1ng/ml TGF-β1 (R&D systems), 20μg/ml anti-IFN-γ and 20μg/ml anti-IL-4. For IL-6 condition, cells were cultured in the presence of 40ng/ml recombinant IL-6, 20μg/ml anti-IFN-γ, 20μg/ml anti-IL-4. 100ng/ml Recombinant Human Activin A (Biolegend) was used in indicated conditions. 10μM TGFβR inhibitor SB525334

(Selleckchem) was added into culture medium with indication of "i". For retroviral transduction, CD4$^+$ T cells were isolated and cultured under various conditions on day 0 and then spin inoculated with indicated retroviruses at 1500g at 30°C for 1.5 hours on day 1. Cells were harvested and analyzed by flow-cytometry on day 4 unless stated otherwise in the figure legends.

Elicitation of experimental autoimmune encephalomyelitis (EAE) in mice

50μg MOG peptide and CFA were emulsified and subcutaneously (i.c.) injected into mice on day 0. 200ng Pertussis toxin was intra-peritoneally (i.p.) injected on day 0 and day 2. Mice were monitored and euthanized at appropriate time. The EAE clinical scores were recorded based on the following criteria: 1. Limp tail; 2. Poor righting ability and/or partial hind-limb paralysis; 3. Total hind-limb paralysis; 4. Hind-limb paralysis + 75% of body paralysis; 5. Moribund; 6. Dead. Seventeen to eighteen days post EAE induction, diseased mice were sacrificed and the spinal cords were subjected to pathological analysis using luxol fast blue staining. Lesions were indicated by the arrows in the figures. T cells from spinal cords were collected and subjected to immunological analysis. For EAE experiments with T cell adoptive transfer, CD4$^+$ T cells of different genotypes or transduced with indicated retrovirus were transferred into $Rag1^{-/-}$ or irradiated WT recipient mice on Day -1. EAE was then elicited in the recipient mice on Day 0. Tamoxifen was injected into the recipient mice on Day 2 and Day 4 to delete floxed alleles in ERCre expressing T cells. Spinal cord lymphocytes were isolated and transferred cells were analyzed by flow-cytometry on day 17 post EAE elicitation.

Immuno-blotting, Immuno-precipitation (IP) and Mass-Spectrometry (MS)

For immuno-blotting, protein extracts were resolved by AnyKD SDS-PAGE gel (Bio-Rad), transferred to a polyvinylidene fluoride membrane (Millipore) and analyzed by immuno-blotting with the following antibodies: anti-Ski (H-329, Santa Cruz), anti-RORγt (B2D, Santa Cruz), anti-Smad4 (D3M6U, CST), anti-pSmad3 (C25A9, CST) and anti-β-actin (I-19, Santa Cruz). For gel source data, see Supplementary Fig. 1.

For IP analysis, cells were lysed with extract buffer (20mM HEPES, pH 7.9, with 1.5mM MgCl$_2$, 0.42 M NaCl, 0.2mM EDTA, and 25% (v/v) Glycerol, 1% Triton X-100) containing protease inhibitor mixture (Roche Applied Science), diluted with 3 volume of dilution buffer (20mM HEPES, pH 7.9, with 1.5mM MgCl$_2$, 0.2mM EDTA, 10mM KCl, and 25% (v/v) Glycerol) and sonicated with Bioruptor PICO. The supernatant were incubated with magnetic beads (Bio-Rad) that had been conjugated with indicated antibody or anti-Flag M2 magnetic beads (Sigma) in cold room overnight. The immunocomplex was washed six times with washing buffer (10mM HEPES, pH 7.9, 1.5mM MgCl$_2$, 0.2mM EDTA and 150mM NaCl) containing 0.1% NP40. Associated proteins were eluted by adding 2× Laemmli sample buffer (Bio-Rad) and incubated at 95°C for 5 min. The eluted proteins were resolved by SDS–PAGE gel for subsequence immuno-blotting or mass-spectrometry.

For MS analysis, CD4$^+$ T cells were cultured in SILAC/AACT L media (RPMI1640 media depletion of lysine and arginine were supplemented with normal L-Lysine (K0)/L-arginine(R0)), or SILAC/AACT H media (RPMI1640 media depletion of lysine and arginine

were supplemented with $^{13}C_6^{15}N_2$-lysine (K8)/$^{13}C_6^{15}N_4$-arginine (R10)). After Immuno-precipitation, eluted proteins were resolved in SDS-PAGE gel and subjected to in-gel digestion with trypsin (Promega) at 37°C. MS analyses of the immuno-precipitation products were performed on a LTQ Orbitrap Velos (Thermo Scientific) coupled with a nanoLC-Ultra system (Eksigent). Samples were re-suspended in 20μl HPLC buffer A (0.1% formic acid in water) and 5μl was loaded onto an IntegraFrit column (C18, New Objective). The peptides were eluted at a flow rate of 250nl/min with a multi-step gradient, 5%–40% buffer B (0.1% formic acid in acetonitrile) for 70 min, 40%–80% buffer B for 5 min, 80% buffer B for 5 min, 80%–5% buffer B for 5 min and 5% buffer B for 5 min. The MS spectra were acquired in a data-dependent and positive ion mode at a spray voltage of 2.1 kV by XCalibur software (version 2.1, Thermo Scientific). Orbitrap analyzer was used to do the survey scan at a resolution of 60,000 at a mass range between m/z 350 and 1,800. The top 11 most intense ions in every cycle were subjected to CID fragmentation in the LTQ Orbitrap with normalized collision energy at 35% and activation Q 0.25. Dynamic exclusion was enabled. MS raw files were analyzed by MaxQuant (version 1.5.0.25). They were searched with Andromeda against Uniprot mouse database (release date: 30 November 2010; 20,248 entries). A database that contains contamination proteins was also used to exclude peptides that matched this database. Searches were performed with a precursor ion mass tolerance of 7.5ppm and MS/MS tolerance at 0.5Da. Peptide and protein identifications were filtered to a maximum 1% and 5% false discovery rate, respectively. Up to two missed cleavages were allowed. Only peptides with a minimum length of seven amino acids were considered for identification. The MS proteomics data have been deposited to the ProteomeXchange Consortium via the PRIDE partner repository with the data set identifier PXD007172.

Chromatin Immuno-precipitation (ChIP) assay

The ChIP assay was done according to the protocol of Upstate Biotechnology. Cells were cross-linked with 1% formaldehyde and lysed in lysis buffer. Lysates were sonicated with Bioruptor PICO or Covaris S220 to shear genomic DNA. Chromatin was subjected to immuno-precipitation overnight at 4°C with anti-H3K9Ac (ab4441, Abcam), anti-IgG (sc-2027, Santa Cruz), anti-Smad4 (EP618Y, Abcam), or anti-Ski (H-329, Santa Cruz). Quantitative real-time PCR was performed to determine the relative abundance of target genomic DNA. Specific PCR primers to detect *Rorc* promoter are: GGGGAGAGCTTTGTGCAGAT and AGTAGGGTAGCCCAGGACAG.

ChIP-seq

The sequencing libraries were prepared by the NEXTflex Rapid DNAseq kit (Bioo Scientific Corporation) and sequenced on NextSeq 500 (Illumina) at the NIEHS Epigenomics Core Facility. Primary data processing: Data were collected using 36 paired-end reads NextSeq 500 platform (Illumina). Raw reads (56–72 Million reads per sample) were first cleaned for adapter sequences using Trim Galore with default parameters. Cleaned reads were aligned to mm10 using Bowtie1 with the parameters -m1, -v2 and –X1500. These parameters ensured that fragments up to 1500bp (-X1500) and mismatch up to 2 (-v2) were allowed to align, and that only unique aligned reads were collected (-m1). For all data files, duplicates were removed using Picard. The ChIP-seq data are available in the Gene Expression Omnibus

repository at the National Center for Biotechnology Information under accession number GSE101593.

RNA-seq

Total RNA was extracted from cells by lysing livers with Trizol (Thermo Fisher Scientific), and purified with the RNeasy mini kit (Qiagen). RNA-seq libraries were generated and poly(A) enriched using 1µg of RNA as input with the TruSeq RNA Sample Prep Kit (Illumina, San Diego, CA).

Indexed samples were sequenced using the 50bp paired-end protocol via the HiSeq 2500 (Illumina) per the manufacturer's protocol. Reads (32–45 Million reads per sample) were aligned to the UCSC mm10 reference genome using STAR with default parameters. The quantification results from featureCounts were then analyzed with the Bioconductor package DESeq2, which fits a negative binomial distribution to estimate technical and biological variability. A gene was considered differentially expressed if the p-value for differential expression was less than 0.05. The RNA-seq data are available in the Gene Expression Omnibus repository at the National Center for Biotechnology Information under accession number GSE101527.

Ski gRNA design for CRISPR/Cas9

gRNAs targeting the first exon of Ski were designed by CHOPCHOP web tool[30]. Two gRNAs of the highest score and specificity were selected based on the algorithm. The sequences for the chosen gRNAs are: gRNA1:GTCTTCTGCAGCCCCGGGTG. gRNA2:GCGAGCTCATGGAGCTCAGG.

Statistical analysis and Reproducibility

Statistical analysis was performed by two-tailed/sided Student's t-test. $p<0.05$ (confidence interval of 95%) was considered statistically significant. In the figures, *, ** and *** were used to indicate $p<0.05$, $p<0.01$ and $p<0.001$ respectively. The exact p values were shown in the source data files. The sample sizes "n" were stated in figure legends to indicate biologically independent replicates used for statistical analysis except for ChIP assay (Fig. 3b, Fig. 4e, Fig. 4f, Extended Data Fig. 2g and Extended Data Fig. 4c) where statistical analysis was performed using independent samples done in one of three independent experiments. Representative results shown in Fig. 1g, 3c, 3d, 3e, 3f and 4g and Extended Data Fig. 2e, 2f, 3b and 3d were from three biologically independent experiments with similar results.

Date availability

The RNA-seq data support the findings of this study have been deposited in the Gene Expression Omnibus repository at the National Center for Biotechnology Information with accession number GSE101527. Fig. 2a and Extended Data Fig. 2b contain RNA-seq related data. The ChIP-seq data support the findings of this study have been deposited in Gene Expression Omnibus repository at the National Center for Biotechnology Information with accession number GSE101593. Fig. 2g and Extended Data Fig. 2h contains ChIP-seq related data. The IP-MS proteomics data support the findings of this study have been deposited in

ProteomeXchange Consortium via the PRIDE partner repository with the data set identifier PXD007172. Extended Data Fig. 3a contains IP-MS related data. All other relevant data are available in the manuscript and from the corresponding author on request.

Extended Data
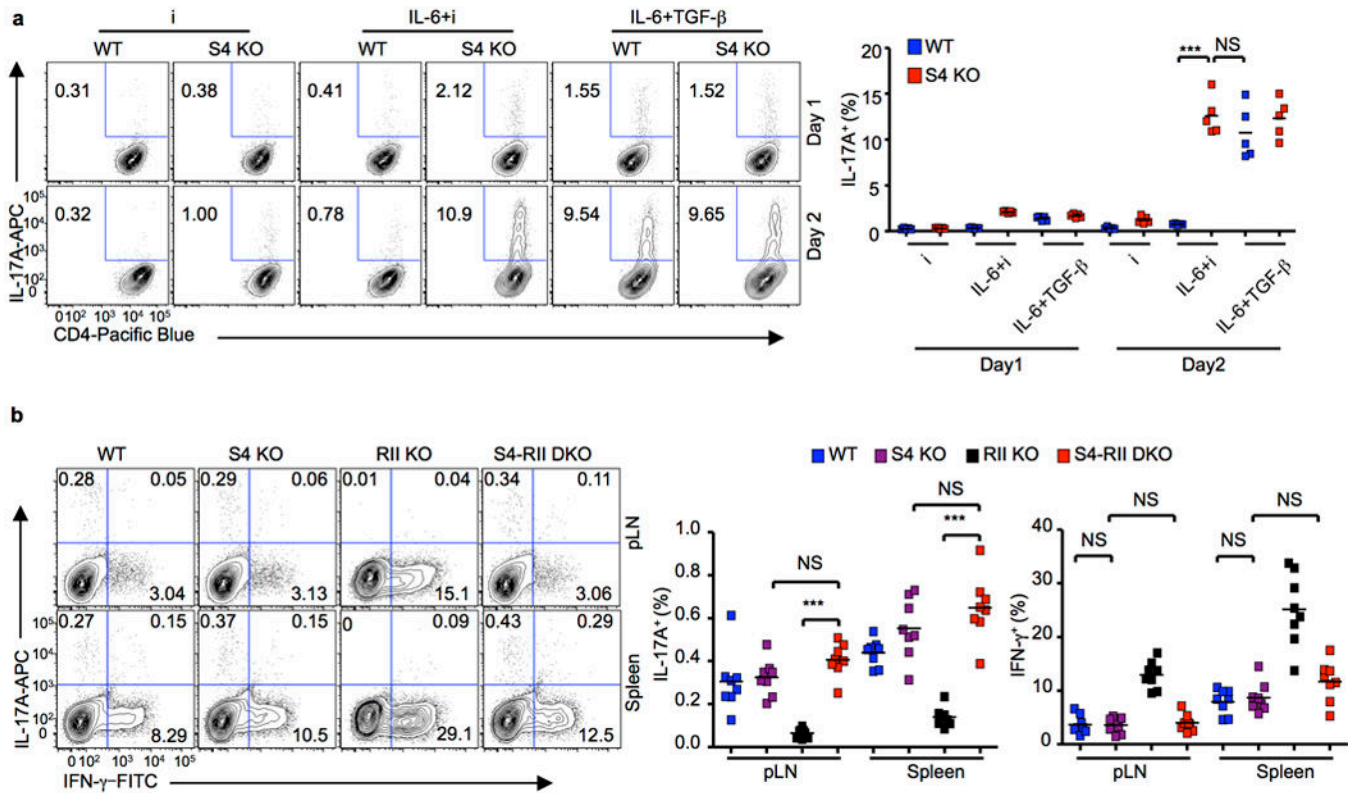
Extended Data Figure 1. Th17 cell differentiation in the absence of Smad4

1a, Naïve CD4+ T cells isolated from WT and *Cd4cre;Smad4*fl/fl (S4 KO) mice were activated in the presence of TGFβR inhibitor (i), IL-6+TGFβR inhibitor (IL-6+i), or IL-6+TGF-β (IL6+TGF-β). IL-17A+ cells were assessed by flow-cytometry 1 and 2 days later. Representative results (left) and statistical analysis (right) of 5 experiments are shown. **1b**, The percentage of IL-17A+CD4+ and IFN-γ+CD4+ cells in the peripheral lymph nodes (pLN) and spleens from WT, *Cd4cre;Smad4*fl/fl (S4 KO), *Cd4cre;Tgfbr2*fl/fl (RII KO) and *Cd4cre;Smad4*fl/fl;*Tgfbr2*fl/fl (S4-RII DKO) mice under steady state were assessed by flow-cytometry. Representative result (left) and statistics from 8 mice (right) are shown. (***p<0.001 per two sided *t*-test; NS, not significant per two-sided *t*-test; centers indicate mean values)
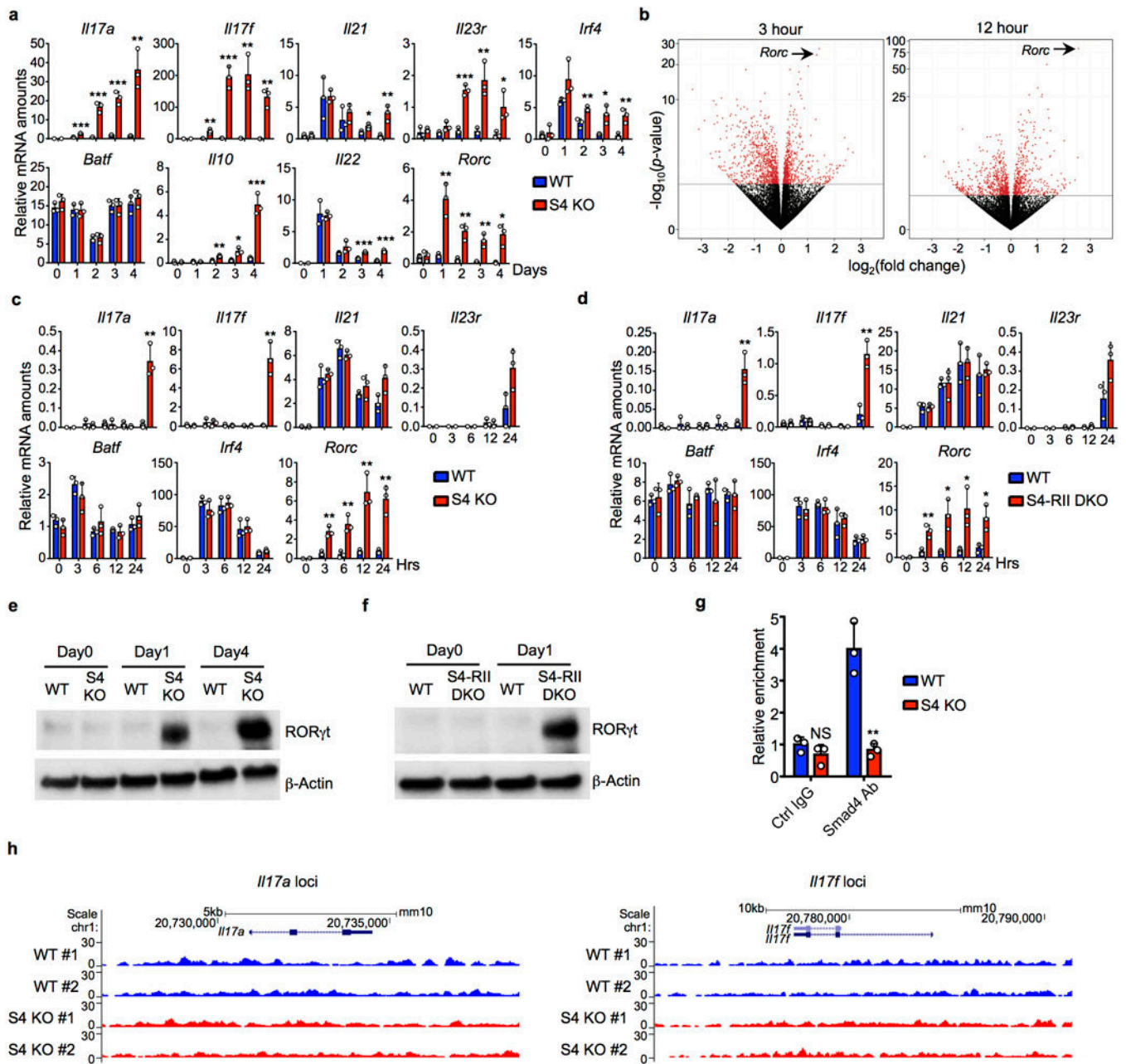
Extended Data Figure 2. Smad4 suppresses RORγt expression

2a, CD4^{+} T cells from WT and *Cd4cre;Smad4*^{fl/fl} (S4 KO) mice were activated in the presence of IL-6 and TGFβR inhibitor. The mRNA expression of Th17 related genes was analyzed at indicated time points post activation by qRT-PCR. Means ± s.d. of three experiments are shown.

2b, Naïve CD4^{+} T cells from WT and *Cd4cre;Smad4*^{fl/fl} (S4 KO) mice were sorted and activated in the presence of IL-6 and TGFβR inhibitor for 3 and 12 hours. Total RNA was then collected for RNA-seq analysis. All genes were analyzed and presented as volcano plots based on the fold change ($\log_2$) of S4 KO versus WT and *p*-value ($-\log_{10}$). Differentially expressed genes ($p<0.05$) are highlighted in red.

2c, Naïve CD4$^+$ T cells from WT and *Cd4cre;Smad4*$^{fl/fl}$ (S4 KO) mice were sorted and activated in the presence of IL-6 and TGFβR inhibitor. The mRNA expression of Th17 related genes was analyzed at indicated time points post activation by qRT-PCR. Means ± s.d. of three experiments are shown.

2d, Naïve CD4$^+$ T cells from WT and *Cd4cre;Smad4*$^{fl/fl}$;*Tgfbr2*$^{fl/fl}$ (S4-RII DKO) mice were sorted and activated in the presence of IL-6. The mRNA expression of Th17 related genes was analyzed at indicated time points post activation by qRT-PCR. Means ± s.d. of three experiments are shown.

2e, Naïve CD4$^+$ T cells from WT and *Cd4cre;Smad4*$^{fl/fl}$ (S4 KO) mice were sorted and activated in the presence of IL-6 and TGFβR inhibitor. The RORγt protein expression was assessed by immuno-blotting 1 and 4 days post activation. Results are representative of three experiments with similar results.

2f, CD4$^+$ T cells from WT and *Cd4cre;Tgfbr2*$^{fl/fl}$;*Smad4*$^{fl/fl}$ (S4-RII DKO) mice were activated in the presence of IL-6. The RORγt protein expression was assessed by immuno-blotting 1 day post activation. Results are representative of three experiments with similar results.

2g, CD4$^+$ T cells from WT and *Cd4cre;Smad4*$^{fl/fl}$ (S4 KO) mice were activated in the presence of IL-6 and TGFβR inhibitor. Cells were harvested after 12 hours. ChIP assay was performed with Ctrl IgG antibody and Smad4 antibody. The enrichment of Smad4 binding to *Rorc* promoter was determined. Means ± s.d. of 3 samples in one experiment of three are shown.

2h, CD4$^+$ T cells from WT and *Cd4cre;Smad4*$^{fl/fl}$ (S4 KO) mice were activated in the presence of IL-6 and TGFβR inhibitor. Cells were harvested after 12 hours. ChIP-seq assay was performed with Smad4 antibody. The enrichment of Smad4 binding to *Il17a and Il17f* loci were determined by the mapped read coverage of Smad4 ChIP-seq data. The results of two independent experiments were show as #1 and #2.

(*p<0.05, **p<0.01, ***p<0.001 per two sided *t*-test; NS, not significant per two-sided *t*-test)
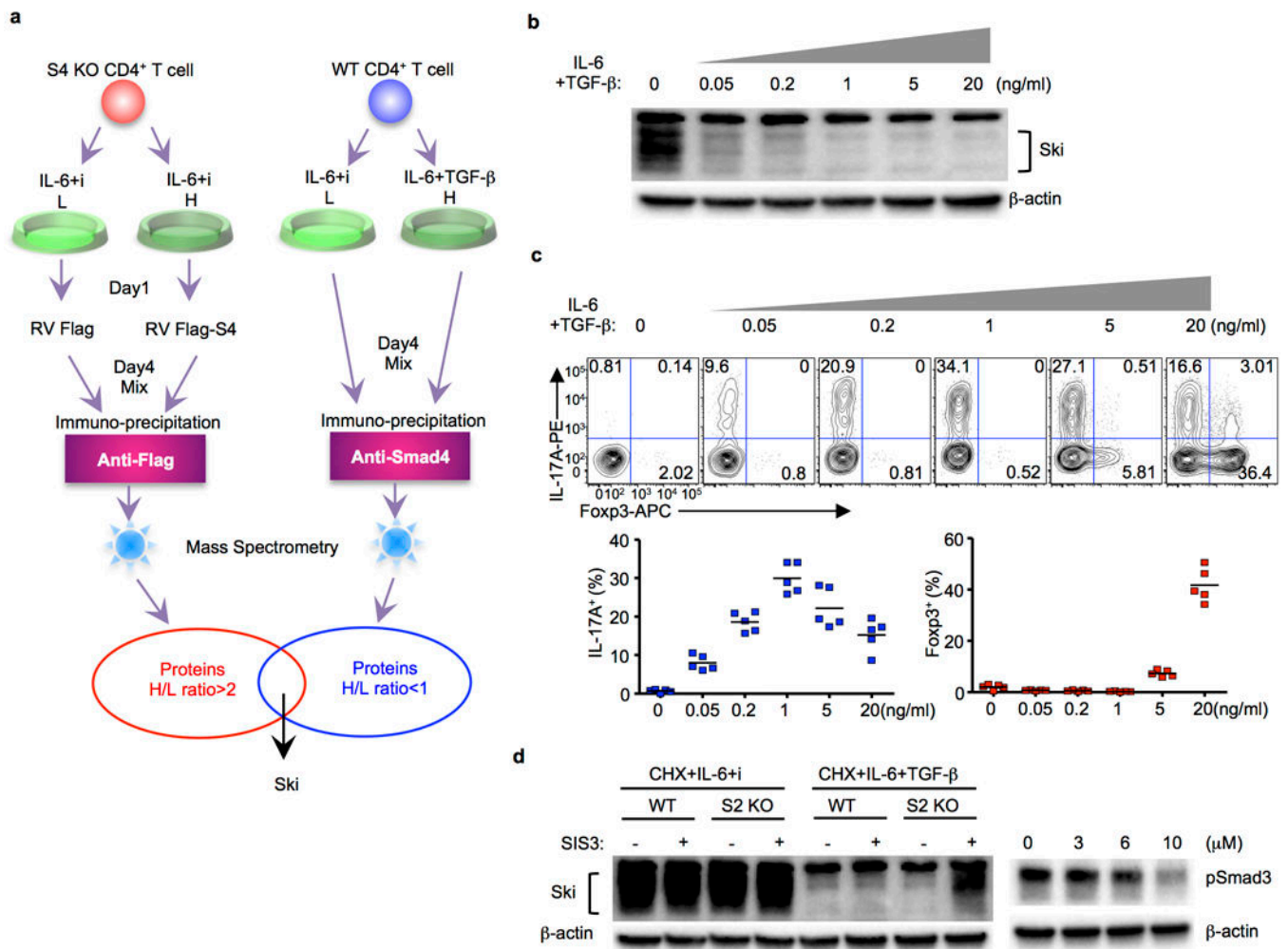
Extended Data Figure 3. Ski identification and its degradation upon low dose of TGF-β

3a, Schematic of quantitative IP-MS (immuno-precipitation and mass spectrometry) proteomic strategy to identify Smad4 binding proteins under different conditions.

In one scheme, to identify Smad4 binding protein in the absence of TGF-β signaling, CD4+ T cell from *Cd4cre;Smad4*^{fl/fl} (S4 KO) mice were sorted and activated in the presence of IL-6+i in the SILAC/AACT medium provided either with amino acids containing light (L) isotopes or with amino acids containing heavy (H) isotopes. Cells were then transduced with retroviruses expressing either Flag tag (RV Flag) or Flag tag and Smad4 fusion protein (RV Flag-S4). Cells were harvested and mixed 4 days post activation. Immuno-precipitation was performed using anti-Flag. IP'ed proteins were processed and subjected to quantitative MS analysis. Proteins with an H/L ratio of more than 2 were identified.

In the other scheme, to identify the proteins whose Smad4 interaction was perturbed upon TGF-β stimulation, CD4+ T cell from WT mice were sorted and activated either in the presence of IL-6+i in the SILAC/AACT medium provided with amino acids containing light (L) isotopes or in the presence of IL-6+TGF-β in the SILAC/AACT medium provided with amino acids containing heavy (H) isotopes. Cells were harvested and mixed on 4 days post activation. Immuno-precipitation was performed using anti-Smad4 antibody. IP'ed proteins

were processed and subjected to quantitative MS analysis. Proteins with an H/L ratio of less than 1 were identified. The commonly identified protein Ski in the two experiments was subjected to further investigation.

3b, CD4^{+} T cell from WT mice were activated in the presence of IL-6 and indicated dose of TGF-β. Cells were harvested after 24 hours. Ski protein expression was detected by immuno-blotting. Results are representative of three experiments with similar results.

3c, CD4^{+} T cell from WT mice were activated in the presence of IL-6 and indicated dose of TGF-β. IL-17A^{+} and Foxp3^{+} cells were assessed by flow-cytometry on day 4. Representative results (upper) and statistical analysis (lower) of 5 experiments are shown (Centers indicate mean values).

3d, CD4^{+} T cells from WT or *Cd4cre;Smad2*^{fl/fl} (S2 KO) mice were activated in the presence of IL-6 for 24 hours. Cells were then stimulated with indicated conditions for additional 1 hour with or without 10μM SIS3 (specific inhibitor of Smad3 phosphorylation). Ski protein expression and Smad3 phosphorylation were assessed by immuno-blotting. Results are representative of three experiments with similar results.
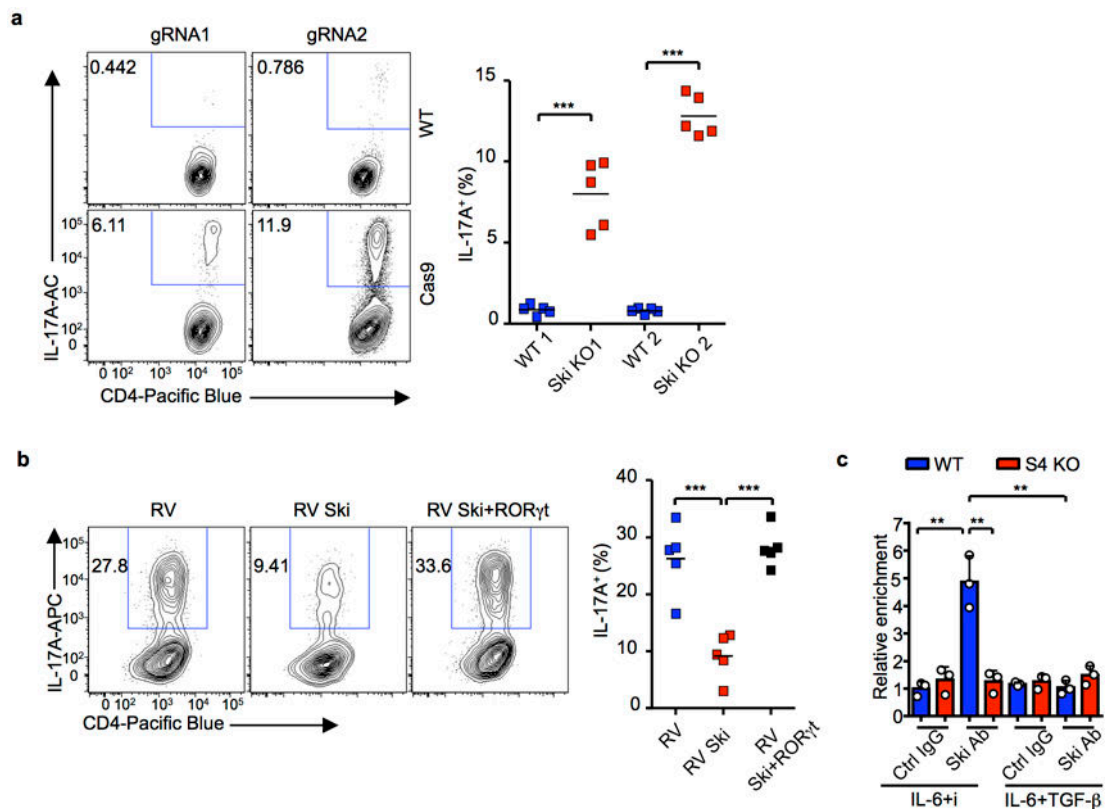
Extended Data Figure 4. Ski and Smad4 cooperatively suppress Th17 differentiation

4a, Bone marrow cells were isolated from the femur bones of sex- and age-matched *Cd4cre;CdC* (Cas9, CD45.2[+]) mice and wild-type (WT, CD45.1[+]) mice. Cells were mixed, and transduced with two different gRNA expressing virus (as indicated) and transferred into sub-lethally irradiated (400 cGy) *Rag1*^{−/−} recipient mice. CD4^{+} T cells isolated from lymph nodes and spleen of generated bone marrow chimeric mice were activated in the presence of IL-6 and TGFβR inhibitor. Cells transduced with gRNA in wild-type donor indicated as WT.

Cells transduced with gRNA in *CD4Cre;CdC* donor indicated as Ski KO. IL-17A⁺ cells were assessed by flow-cytometry on day 4. Representative results (left) and statistical analysis (right) of 5 experiments are shown.

4b, CD4⁺ T cells from WT mice were activated in the presence of IL-6 and TGF-β, and then transduced with MSCV-IRES-GFP (RV), MSCV-Ski-IRES-GFP (RV Ski) or co-transduced with MSCV-Ski-IRES-GFP and MSCV-RORγt-IRES-Thy1.1 (RV Ski+RORγt) retroviruses. IL-17A expression of transduced (GFP⁺) or co-transduced (GFP⁺Thy1.1⁺) T cells was assessed by flow-cytometry. Representative results (left) and statistical analysis (right) of 5 experiments are shown.

4c, CD4⁺ T cells from WT and *Cd4cre;Smad4*^fl/fl (S4 KO) mice were activated in the presence of IL-6+TGFβR inhibitor (i) or IL-6+TGF-β. Cells were harvested 3 days later. ChIP assay was performed with Control IgG antibody or Ski antibody. The relative enrichment of Ski binding to *Rorc* locus was determined. Means ± s.d. of 3 samples in one experiment of three are shown.

(**P<0.01, ***P<0.001 per two sided *t*-test; NS, not significant per two sided *t*-test; centers indicate mean values)
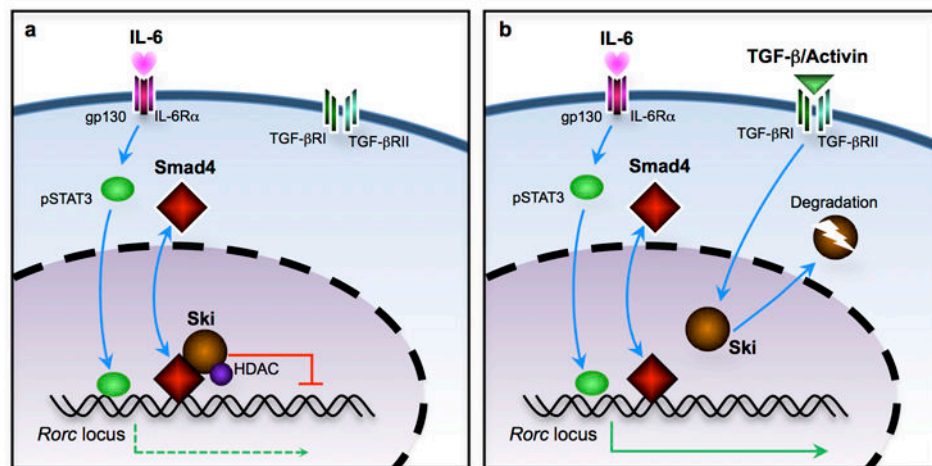
Extended Data Figure 5. TGF-β superfamily signaling overcomes Ski-Smad4 complex mediated suppression of RORγt expression in activated T cells to license Th17 cell differentiation
5a, RORγt expression is potentiated by IL-6-STAT3 signaling but restrained by the HDAC-activity-containing Ski-Smad4 complex that associates with and de-acetylates *Rorc* locus.
5b, Additional TGF-β or Activin signaling triggers Ski degradation. The disruption of Ski-Smad4 complex dissociates HDAC activity from *Rorc* locus and to license RORγt expression and Th17 cell differentiation.

Supplementary Material

Refer to Web version on PubMed Central for supplementary material.

Acknowledgments

References

1. Weaver CT, Hatton RD, Mangan PR, Harrington LE. IL-17 family cytokines and the expanding diversity of effector T cell lineages. Annu Rev Immunol. 2007; 25:821–852. [PubMed: 17201677]

2. Korn T, Bettelli E, Oukka M, Kuchroo VK. IL-17 and Th17 Cells. Annu Rev Immunol. 2009; 27:485–517. [PubMed: 19132915]

3. Miossec P, Korn T, Kuchroo VK. Interleukin-17 and type 17 helper T cells. The New England journal of medicine. 2009; 361:888–898. [PubMed: 19710487]

4. Singh RP, et al. Th17 cells in inflammation and autoimmunity. Autoimmunity reviews. 2014

5. Patel DD, Kuchroo VK. Th17 Cell Pathway in Human Immunity: Lessons from Genetics and Therapeutic Interventions. Immunity. 2015; 43:1040–1051. [PubMed: 26682981]

6. Bettelli E, et al. Reciprocal developmental pathways for the generation of pathogenic effector TH17 and regulatory T cells. Nature. 2006; 441:235–238. [PubMed: 16648838]

7. Veldhoen M, Hocking RJ, Atkins CJ, Locksley RM, Stockinger B. TGFbeta in the context of an inflammatory cytokine milieu supports de novo differentiation of IL-17-producing T cells. Immunity. 2006; 24:179–189. [PubMed: 16473830]

8. Mangan PR, et al. Transforming growth factor-beta induces development of the T(H)17 lineage. Nature. 2006; 441:231–234. [PubMed: 16648837]

9. Manel N, Unutmaz D, Littman DR. The differentiation of human T(H)-17 cells requires transforming growth factor-beta and induction of the nuclear receptor RORgammat. Nature immunology. 2008; 9:641–649. [PubMed: 18454151]

10. Volpe E, et al. A critical function for transforming growth factor-beta, interleukin 23 and proinflammatory cytokines in driving and modulating human T(H)-17 responses. Nature immunology. 2008; 9:650–657. [PubMed: 18454150]

11. Gu AD, et al. A critical role for transcription factor Smad4 in T cell function that is independent of transforming growth factor beta receptor signaling. Immunity. 2015; 42:68–79. [PubMed: 25577439]

12. Yang XO, et al. Molecular antagonism and plasticity of regulatory and inflammatory T cell programs. Immunity. 2008; 29:44–56. [PubMed: 18585065]

13. Lee PP, et al. A Critical role for Dnmt1 and DNA methylation in T cell development, function, and survival. Immunity. 2001; 15:763–774. [PubMed: 11728338]

14. Chu GC, Dunn NR, Anderson DC, Oxburgh L, Robertson EJ. Differential requirements for Smad4 in TGFbeta-dependent patterning of the early mouse embryo. Development. 2004; 131:3501–3512. [PubMed: 15215210]

15. Chytil A, Magnuson MA, Wright CV, Moses HL. Conditional inactivation of the TGF-beta type II receptor using Cre:Lox. Genesis. 2002; 32:73–75. [PubMed: 11857781]

16. Shapiro-Shelef M, Lin KI, Savitsky D, Liao J, Calame K. Blimp-1 is required for maintenance of long-lived plasma cells in the bone marrow. J Exp Med. 2005; 202:1471–1476. [PubMed: 16314438]

17. Massague J. TGFbeta signalling in context. Nat Rev Mol Cell Biol. 2012; 13:616–630. [PubMed: 22992590]

18. Wang T, Gu S, Ronni T, Du YC, Chen X. In vivo dual-tagging proteomic approach in studying signaling pathways in immune response. Journal of proteome research. 2005; 4:941–949. [PubMed: 15952741]

19. Deheuninck J, Luo K. Ski and SnoN, potent negative regulators of TGF-beta signaling. Cell research. 2009; 19:47–57. [PubMed: 19114989]

20. Colmenares C, et al. Loss of the SKI proto-oncogene in individuals affected with 1p36 deletion syndrome is predicted by strain-dependent defects in Ski–/– mice. Nature genetics. 2002; 30:106–109. [PubMed: 11731796]

21. Doyle AJ, et al. Mutations in the TGF-beta repressor SKI cause Shprintzen-Goldberg syndrome with aortic aneurysm. Nature genetics. 2012; 44:1249–1254. [PubMed: 23023332]

22. Sun Y, Liu X, Ng-Eaton E, Lodish HF, Weinberg RA. SnoN and Ski protooncoproteins are rapidly degraded in response to transforming growth factor beta signaling. Proc Natl Acad Sci U S A. 1999; 96:12442–12447. [PubMed: 10535941]

23. Wu JW, et al. Structural mechanism of Smad4 recognition by the nuclear oncoprotein Ski: insights on Ski-mediated repression of TGF-beta signaling. Cell. 2002; 111:357–367. [PubMed: 12419246]

24. Nomura T, et al. Ski is a component of the histone deacetylase complex required for transcriptional repression by Mad and thyroid hormone receptor. Genes & development. 1999; 13:412–423. [PubMed: 10049357]

25. Heldin CH, Miyazono K, ten Dijke P. TGF-beta signalling from cell membrane to nucleus through SMAD proteins. Nature. 1997; 390:465–471. [PubMed: 9393997]

26. Laurence A, et al. Interleukin-2 signaling via STAT5 constrains T helper 17 cell generation. Immunity. 2007; 26:371–381. [PubMed: 17363300]

27. Yang XO, et al. STAT3 regulates cytokine-mediated generation of inflammatory helper T cells. J Biol Chem. 2007; 282:9358–9363. [PubMed: 17277312]

28. Durant L, et al. Diverse targets of the transcription factor STAT3 contribute to T cell pathogenicity and homeostasis. Immunity. 2010; 32:605–615. [PubMed: 20493732]

29. Platt RJ, et al. CRISPR-Cas9 knockin mice for genome editing and cancer modeling. Cell. 2014; 159:440–455. [PubMed: 25263330]

30. Labun K, Montague TG, Gagnon JA, Thyme SB, Valen E. CHOPCHOP v2: a web tool for the next generation of CRISPR genome engineering. Nucleic Acids Res. 2016; 44:W272–276. [PubMed: 27185894]
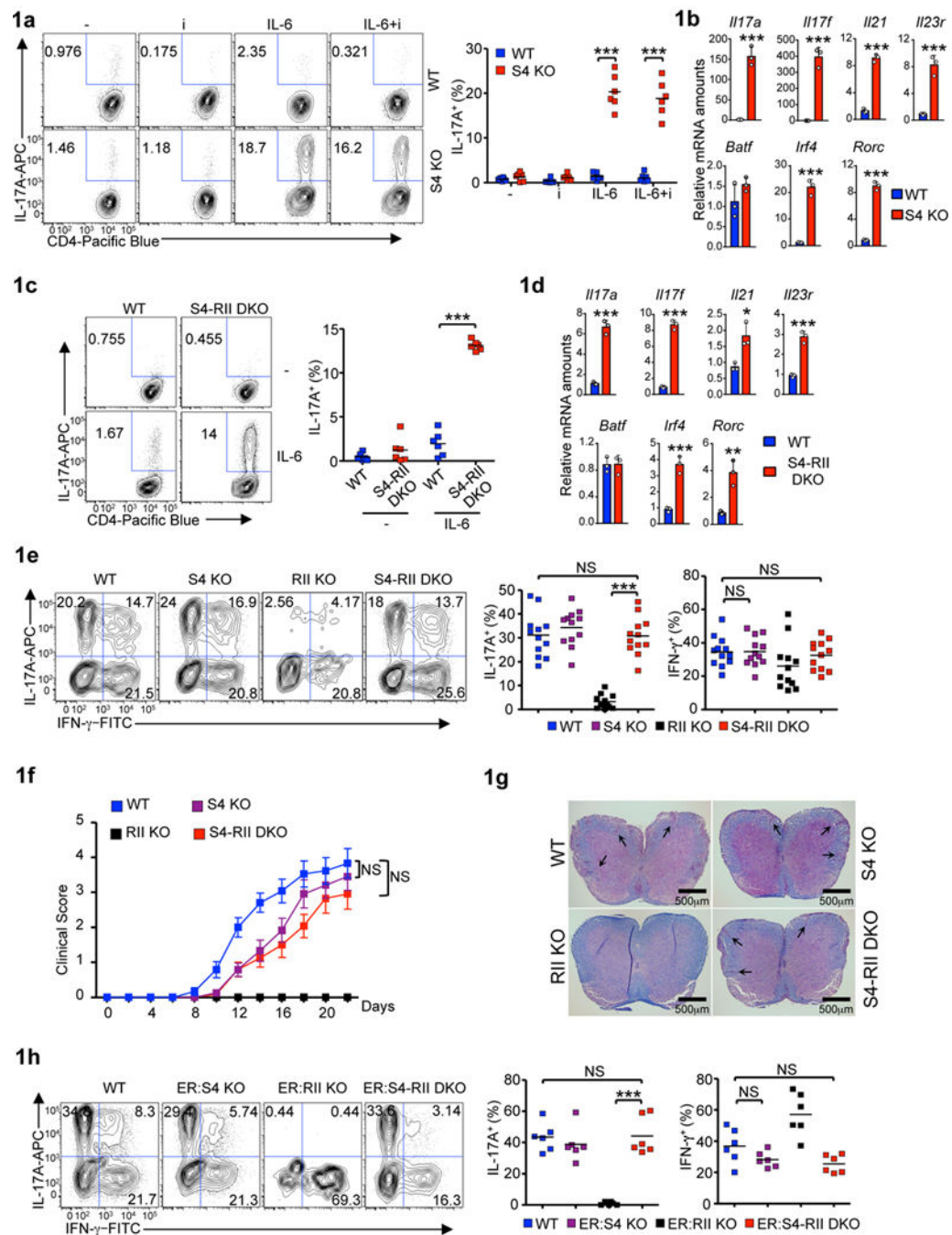
Figure 1. Smad4 deletion leads to a Th17 differentiation in the absence of TGF-β signaling

a, c, Flow-cytometry of cells cultured with or without TGFβR inhibitor (i) (n=6 experiments). **b,d**, qRT-PCR of cells cultured with IL-6+i (b) or IL-6 (d) for 4 days (n=3 experiments, mean ± s.d.). **e-g**, Flow-cytometry of spinal-cord-infiltrating cells (e), clinical scores (f) of EAE-inflicted mice (n=12 each group, mean ± s.e.m.), representative pathology (g, n=3 experiments, scale bar 500μm). **h**, Flow-cytometry of spinal-cord-infiltrating, transferred cells in EAE mice (n=6 each group). (NS, not significant, *p<0.05, **p<0.01, ***p<0.001 per two-sided t-test; centers indicate mean values)
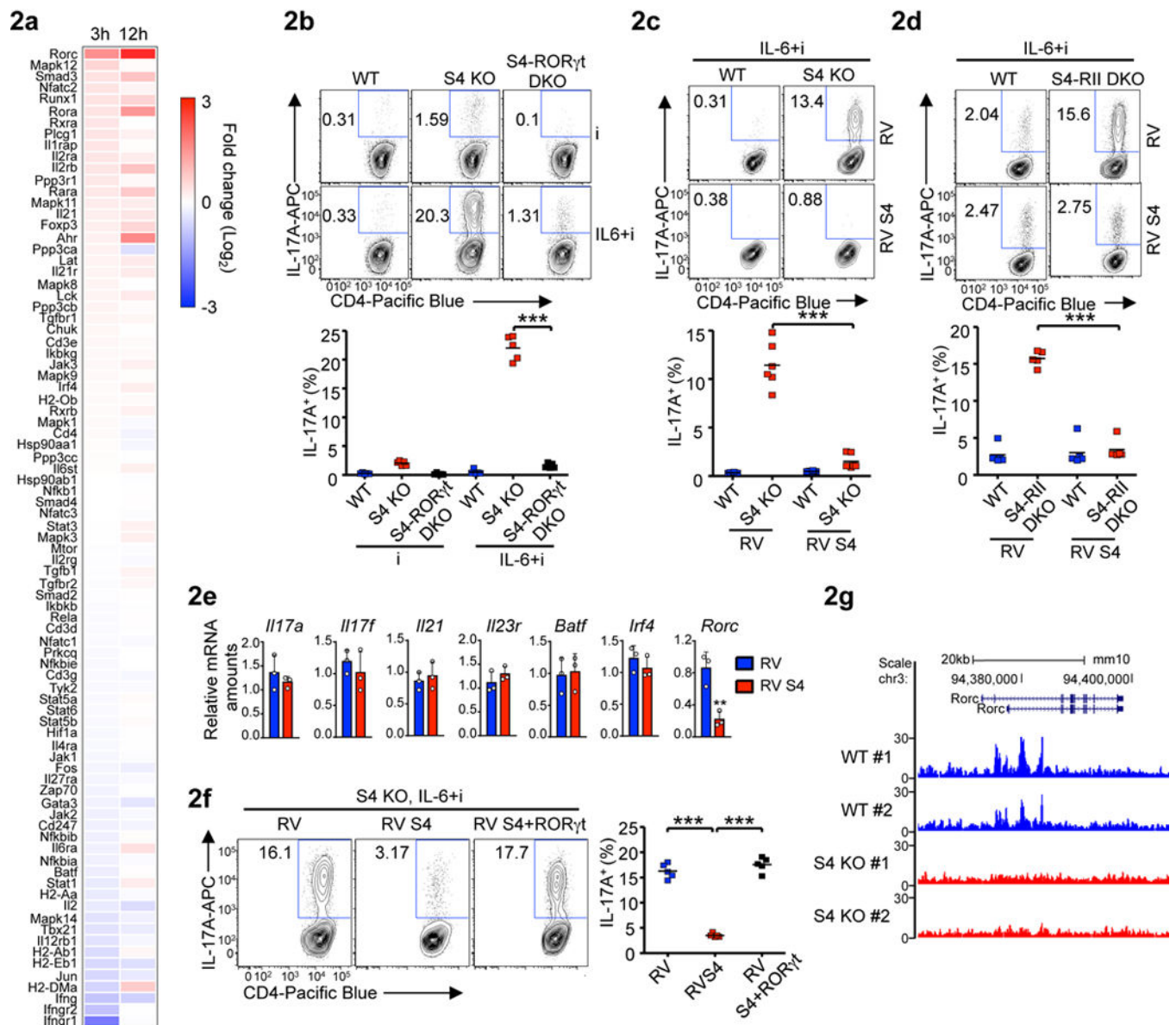
Figure 2. Smad4 controls Th17 cell program by directly suppressing *Rorc* expression

a, Differential expression of S4 KO/WT cells cultured with IL-6+TGFβR inhibitor by RNA-seq (scale bar is indicated). **b-d,f**, Flow-cytometry of cells without (b) or with (c, d, f) retrovirus (RV) transduction (n=5 experiments in b, d, f, n=6 experiments in c). **e**, qRT-PCR of S4 KO cells cultured with IL-6+TGFβR inhibitor, 18-hour post retrovirus transduction (n=3 experiments, mean ± s.d.). **g**, ChIP-seq analysis of Smad4 binding at *Rorc* locus in cells cultured with IL-6+TGFβR inhibitor for 24 hours (n=2 experiments). (**p<0.01, ***p<0.001 per two-sided t-test; centers indicate mean values)
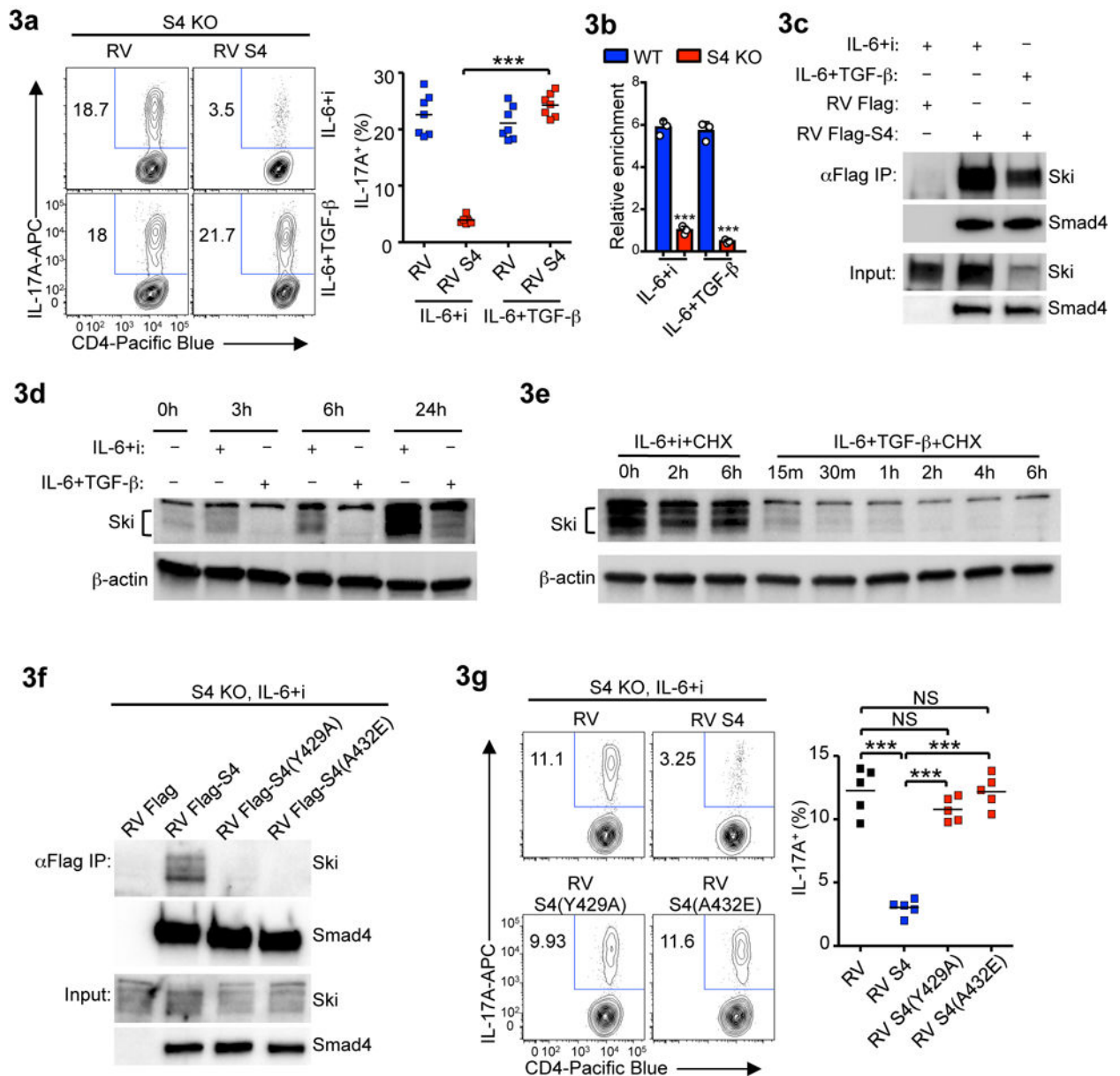
Figure 3. TGF-β signaling disrupts Ski-Smad4 complex to license Th17 differentiation

a, g Flow-cytometry of cells transduced with retrovirus expressing wild-type or mutant Smad4 (n=7 experiments in a; n=5 experiments in g). **b**, ChIP of Smad4 binding at *Rorc* promoter (n=3 samples, mean ± s.d.). **c-f**, Immuno-precipitation and immune-blotting of S4 KO (c, f) or WT (d, e) cells treated as indicated (n=3 experiments). In e, cells were pre-cultured with IL-6 for 24 hours. (NS, not significant, ***$p<0.001$ per two-sided t-test; centers indicate mean values)
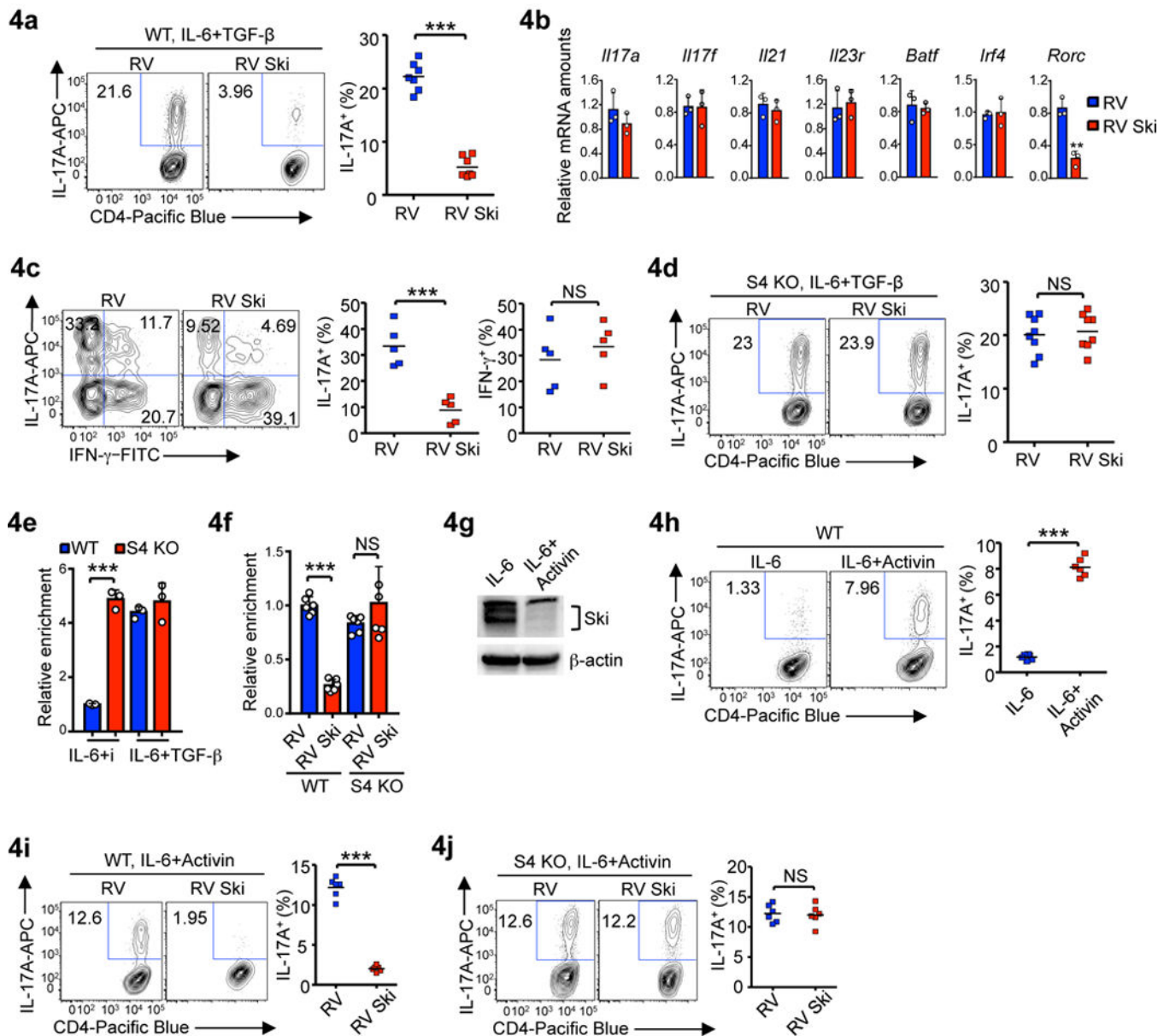
Figure 4. Ski suppresses Th17 differentiation in a Smad4-dependent manner
a, d, h-j, Flow-cytometry of cultured cells (n=7 in a, n=8 in d and n=6 in h-j experiments). **b**, qRT-PCR of WT cells cultured with IL-6+TGF-β, 18-hour post retrovirus transduction (n=3 experiments, mean ± s.d.). **c**, Flow-cytometry of spinal-cord-infiltrating, transferred cells in EAE mice (n=5). **e, f**, ChIP of H3K9Ac at *Rorc* promoter (n=3 samples in e; n=6 samples in f, mean ± s.d.). **g**, Immune-blotting of WT cells cultured for 24 hours (n=3 experiments). (NS, not significant, **p<0.01, ***p<0.001 per two-sided t-test; centers indicate mean values)